Experimental study of exiton binding energy in semiconducting carbon nanotubes

Nicolas Izard,[1,2,*] Etienne Gaufrès,[1] Xavier Le Roux,[1] Saïd Kazaoui,[2]
Yoishi Murakami (村上陽一),[3] Delphine Marris-Morini,[1] Eric
Cassan,[1] Shigeo Maruyama (丸山茂夫),[4] and Laurent Vivien[1,†]

[1]*Institut d'Electronique Fondamentale, CNRS-UMR 8622,*
Univ. Paris-Sud, 91405 Orsay, France
[2]*National Institute of Advance Industrial Science*
and Technology (AIST), Tsukuba 305-8565, Japan
[3]*Global Edge Institute, Tokyo Institute of Technology, Tokyo, Japan*
[4]*Departement of Mechanical Engineering,*
The University of Tokyo, Tokyo, Japan

(Dated: July 21, 2010)

Abstract

Electroabsorption spectroscopy of well identified index-defined semiconducting carbon nanotubes is reported. The measurement of high definition electroabsorption spectrum allows an direct indexation with unique nanotube chirality. Results show that the electroabsorption is directly proportional to the exciton binding energy of nanotubes. Electroabsorption is a powerfull technique which directly probe into carbon nanotubes excitonic states, and may become a usefull tool for in-situ study of excitons in future nanotube based photonic devices.

PACS numbers: 78.67.Ch, 78.20.Jq, 73.22.-f

Keywords: nanotube; electromodulation

I. INTRODUCTION

Single Wall Carbon Nanotubes (SWNT) are nano-sized unidimensional structures which have been extensively studied in the past ten years for their very peculiar electrical and optical properties. Semiconducting single wall carbon nanotubes (s-SWNT), with their direct band-gap, present special interest for nanophotonic and electro-optic applications[1,2]. Electron confinement in one dimensional nanotube leads to strong electron-hole localization, with binding energy as high as 0.5 eV, and the formation of the so-called excitonic states[3]. Exciton binding energy strongly depends on the nanotube intrinsic parameters (diameter, chirality)[4] and on external parameters such as strain[5,6] or the dielectric constant of the surrounding medium[7,8]. Therefore, one can use the environnement to tailor s-SWNT optical properties, and on the other hand, the changes in the environment could strongly affect s-SWNT properties, making them very efficient sensors[9]. As excitonic processes are fundamental, numerous studies buckle down to elucidate them. Usually, excitons could be classified under two categories, dipole-allowed "bright" excitons and dipole-forbidden "dark" excitons, the sooner being probed by linear absorption spectra while dark excitonic states with non-zero momentum are probed by two-photon absorption spectroscopy[3]. In contrary, electroabsorption (EA) spectroscopy allows access to the full nanotube excitonic states, and is directly related to excitonic binding energy[10,11].

Experimentally, EA spectroscopy of carbon nanotubes is quite challenging due to mixing of metallic and semiconducting nanotubes and often because of mutually overlapped absorptions of different chirality tubes having proximate excitonic energies[12]. However, recent advances in SWNT separation techniques, either by density gradient ultracentrifugation[13,14] or by polymer-assisted extraction[15,16], now allow to obtain well defined semiconducting nanotubes with a limited extent of chiral index without detectable traces of metallic nanotubes[17]. In this paper, we report the direct study of excitonic binding energy in well index-defined s-SWNT using EA spectroscopy, which give new insights into s-SWNT electronic structure and exitonic states.

II. MATERIALS AND EXPERIMENTAL DETAILS

The current study uses two different kinds of s-SWNT, both prepared using a polymer assisted selective extraction technique[17]. The first sample was made to be as close as possible to a single index nanotube distribution. A narrow diameter SWNT distribution synthesized by the CoMoCAT process (from SouthWest NanoTech. Inc.) was used as a starting material. This raw material was dispersed with poly-9,9-di-n-octyl-fluorenyl-2,7-diyl (PFO) polymer in a toluene / acetic acid solution using sonication, and, after an ultracentrifugation step, leads to sample “CoMoCAT/PFO” constituting almost exclusively of (7,5) chirality s-SWNT[18].

The second sample was made such as to have the widest possible range of s-SWNT chiralities, but at the same time having a distribution of well defined single chirality peaks. For that purpose, a large diameter SWNT distribution of as-prepared HiPCO SWNT powder (from Unidym Inc.) was used as a starting material. Details of this sample preparation procedure are reported elsewhere[17]. Briefly, the preparation procedure involves an homogeneization step (1 h with a water-bath sonicator and 15 min with a tip sonicator) of the PFO-SWNT mixture, followed by an ultracentrifugation step (2 h, 150.000 g). This method leads to sample “HiPCO/PFO”, with a majority of (8,6), (8,7) and (7,6) s-SWNT chiralities, as well as few (7,5) and (9,7) chiralities[19,20].

Both samples were drop casted on a 2x2 mm quartz substrate, with 100 μm spaced interdigitated Cr/Au electrodes prealably deposited. s-SWNT doped thin layers were subsequently annealed at 180°C for 15 min, resulting in highly fluorescent layers, with an homogeneous s-SWNT density[2].

Electromodulation spectroscopy experiments were then made. Sample was set inside a vacuum chamber (10^{-5} torr) to prevent air breakdown under high electric fields. The light source was a high power Halogen/Xenon white lamp, with a Nikkon monochromator. Electrical modulation was assured by a function generator at a frequency f of 333 Hz, with a voltage amplification up to 300 V. Liquid nitrogen cooled Si and Ge detectors were used for the detection of the doubled frequence ($2f$) component. We experimentally obtained the variation of transmission $-\Delta T$ which could be related to the change in absorption $\Delta\alpha$ by the relation: $\Delta\alpha = \frac{-\Delta T}{T}$.

III. RESULTS AND DISCUSSION

Room temperature electroabsorption spectrum (EA) of CoMoCAT/PFO at 12 kV/cm is reported in Fig. 1a, while the corresponding absorption spectrum is reported in Fig. 1b. A striking feature in the EA spectrum is the unique and well defined peak at 1.18 eV. Interestingly, there is a corresponding feature in the absorption spectrum, also at 1.18 eV. The CoMoCAT/PFO absorption spectra is mainly constituted by two main peaks at 1.18 eV and 1.9 eV. Those peaks correspond to the E_{11} and E_{22} optical exciton transitions, below the Δ_{11} and Δ_{22} continuums. Using well-known assignation rules[21], one can assigned the observed excitonic transitions to index defined nanotubes. In the case of CoMoCAT/PFO sample, peaks at 1.18 eV and 1.9 eV could be respectively attributed to the (7,5)'s E_{11} and the (7,5)'s E_{22} excitons. The other two small features around 1.24 eV and 1.4 eV are attributed to trace of different nanotubes, probably (6,5) and (6,4) s-SWNT. So, the observed peak in the EA spectrum could be assigned to the (7,5) SWNT first exciton.

In order to further investigate the origin of this EA peak, a serie of EA spectrum were performed on sample CoMoCAT/PFO while varying the applied field from 6 to 16.5 kV/cm. Below 6 kV/cm, the EA signal was hardly distinguishable from noise while above 16.5 kV/cm the voltage amplification system saturates. The (7,5) s-SWNT EA peak was fitted by a single lorenzian, and amplitude $\Delta\alpha$, peak position and its full width half maximum (FWHM) were extracted. Peak amplitude as a function of the square electrical field F^2 is displayed on Fig. 2a, while peak position and FWHM as a function of the electrical field F are displayed in Fig. 2b and c, respectively.

No significant peak shift or peak broadening could be detected while applying the electrical field from 6 to 16.5 kV/cm. This means that the field applied to the system remains low, and that the excitonic dissociation is negligible. In that case, EA theory[10,11] states that $\Delta\alpha$ obey the following relation:

$$\Delta\alpha = \frac{K}{E_b} \cdot d_t \cdot F^2 \tag{1}$$

where E_b is the excitonic binding energy, d_t the SWNT diameter, F the applied electric field, and K a constant. As in the current case there is only one kind of nanotube, E_b and d_t are both constant, and $\Delta\alpha$ should be directly proportional to F^2, which is what was experimentally obtained (Fig. 2a). This demonstrate that the observed EA peak at 1.18 eV in Fig. 1a is from excitonic origin.

Relations between nanotube diameter and EA spectrum were also investigated. Previously prepared HiPCO/PFO sample, which contains several well identified s-SWNT chiralities with well separated absorption features, is ideal for that study. Room temperature EA spectrum at 12 kV/cm and the corresponding absorption spectrum are reported in Fig. 3.

EA spectrum is mainly constituted of five peaks, with five corresponding peaks in the absorption spectrum. As previously done, it is possible to assign optical transitions to individual s-SWNT E_{11} excitons, ranging from (7,5) to (9,7) s-SWNT, with diameter ranging from 0.83 to 1.10 nm. As the absorption peaks of HiPCO/PFO sample are well separated from each others, the resulting EA spectrum is constituted by the individual contribution from those five s-SWNT, making it straightforward to assignate EA peaks. An asymmetry could be observed on all EA peaks in HiPCO/PFO sample, as well as to a lesser extent in CoMoCAT/PFO sample. This effect is particularly clear with the (8,6) EA peak at 1.039 eV, which is very intense with a clear asymetric feature at lower energy. This asymetric feature in EA peaks is expected by theoretical results from Zhao et al.[10], and our experimental results are in good agreement with thoses calculations.

An interesting way to analyse EA relations with s-SWNT diameter consists to normalize EA amplitude $\Delta\alpha$ at a given field by the absorption amplitude α for each nanotube. Indeed, this give the intrinsic EA response of each s-SWNT independently from it concentration in samples. Plot of this normalized EA amplitude as the function of the nanotube diameter is reported in Fig. 4. Exciton binding energy E_b could be given by the following analytical expression from Capaz et al.[22]:

$$E_b = \frac{1}{d_t}\left(A + \frac{B}{d_t} + C\zeta + D\zeta^2\right) \tag{2}$$

where d_t is the tube diameter and $\zeta = (-1)^\nu \cos 3\theta / d_t$ represents the chirality dependence. A, B, C and D are numerical constants, and their value are respectively $A = 0.6724$ eV nm, $B = -4.910$ x 10^{-2} eV nm^2, $C = 4.577$ x 10^{-2} eV nm^{-2} and $D = -8.325$ x 10^{-3} eV nm^3.

Exciton binding energy for the five s-SWNT that we had measured normalized EA amplitude were calculated using Eq. 2 and reported in Fig. 4. Normalised EA response is in very good agreement with the calculated exciton binding energy, and normalised EA response $\Delta\alpha/\alpha$ is directly proportional to the exciton binding energy E_b^{11}. Therefore, electroabsorption spectroscopy is a powerfull technique to directly probe exciton binding energy in carbon nanotubes, and may become a usefull experimental tool to investigate modification of E_b^{11}

under changes in surrounding medium or chemical functionalization.

IV. SUMMARY

We report the first electroabsorption experiments performed on well identified index-defined semiconducting nanotubes. The electroabsorption response is defined enough to allow a peak-to-peak correspondence with the absorption spectrum, leading to an unprecedented indexation of electroabsorption spectrum. Due to its excitonic nature, electroabsorption amplitude is quadratic with the applied electric field. Our results show that electroabsorption is proportional with exciton binding energy, in good agreement with theoretical works. Electroabsorption is an interesting technique to directly probe excitons in carbon nanotube. From that aspect, EA can prove to be an invaluable tool for the direct study of excitonic-based effects in future carbon nanotubes based photonics devices.

ACKNOWLEDGMENTS

N. Izard thanks the Japan Society for the Promotion of Science and CNRS for financial support.

---

[*] nicolas.izard@u-psud.fr; http://silicon-photonics.ief.u-psud.fr

[†] laurent.vivien@u-psud.fr

[1] P. Avouris, J. Chen, M. Freitag, V. Perebeinos, and J. Tsang, Phys. Stat. Sol. B, **243**, 3197 (2006).

[2] E. Gaufrès, N. Izard, X. Le-Roux, D. Marris-Morini, S. Kazaoui, E. Cassan, and L. Vivien, Appl. Phys. Lett., **96**, 231105 (2010).

[3] F. Wang, G. Dukovic, L. Brus, and T. Heinz, Science, **308**, 838 (2005).

[4] S. Lebedkin, F. Hennrich, O. Riowski, and M. Kappes, Phys. Rev. B, **77**, 165429 (2008).

[5] L. Yang and J. Han, Phys. Rev. Lett., **85**, 154 (2000).

[6] T. Leeuw, D. Tsyboulski, P. Nikolaev, S. bachilo, S. Arepalli, and R. Weisman, Nano Letters, **8**, 826 (2008).

[7] J. Lefebvre, J. Fraser, Y. Homma, and P. Finnie, Appl. Phys. A, **78**, 1107 (2004).

[8] N. Izard, D. Riehl, and E. Anglaret, Phys. Rev. B, **71**, 195417 (2005).

[9] J. Kong, N. Franklin, C. Zhou, M. Chapline, S. Peng, K. Cho, and H. Dai, Science, **287**, 622 (2000).

[10] H. Zhao and S. Mazumdar, Phys. Rev. Lett., **98**, 166805 (2007).

[11] V. Perebeinos and P. Avouris, Nano Letters, **7**, 609 (2007).

[12] H. Kishida, Y. Nagasawa, S. Imamura, and A. Nakamura, Phys. Rev. Lett., **100**, 097401 (2008).

[13] M. Arnold, S. Stupp, and M. Hersam, Nano Letters, **5**, 713 (2005).

[14] S. Ghosh, S. M. Bachilo, and R. B. Weisman, Nature Nanotechnology, **5**, 443 (2010).

[15] A. Nish, J.-Y. Hwang, J. Doig, and R. Nicholas, Nature Nanotechnology, **2**, 640 (2007).

[16] F. Chen, B. Wang, Y. Chen, and L.-J. Li, Nano Letters, **7**, 3013 (2007).

[17] N. Izard, S. Kazaoui, K. Hata, T. Okazaki, T. Saito, S. Iijima, and N. Minami, Appl. Phys. Lett., **92**, 243112 (2008).

[18] Y. Murakami, B. Lu, S. Kazaoui, N. Minami, T. Okubo, and S. Maruyama, Phys. Rev. B, **79**, 195407 (2009).

[19] E. Gaufrès, N. Izard, L. Vivien, S. Kazaoui, D. Marris-Morini, and E. Cassan, Opt. Lett., **34**, 3845 (2009).

[20] E. Gaufrès, N. Izard, X. Le-Roux, D. Marris-Morini, S. Kazaoui, E. Cassan, and L. Vivien, Opt. Express, **18**, 5740 (2010).

[21] M. J. O'Connell, S. M. Bachilo, C. B. Huffman, V. C. Moore, M. S. Strano, E. H. Haroz, K. L. Rialon, P. J. Boul, W. H. Noon, C. Kittrell, J. Ma, R. H. Hauge, R. B. Weisman, and R. E. Smalley, Science, **297**, 593 (2002).

[22] R. B. Capaz, C. D. Spataru, S. Ismail-Beigi, and S. G. Louie, Phys. Rev. B, **74**, 121401 (2006).

FIGURES

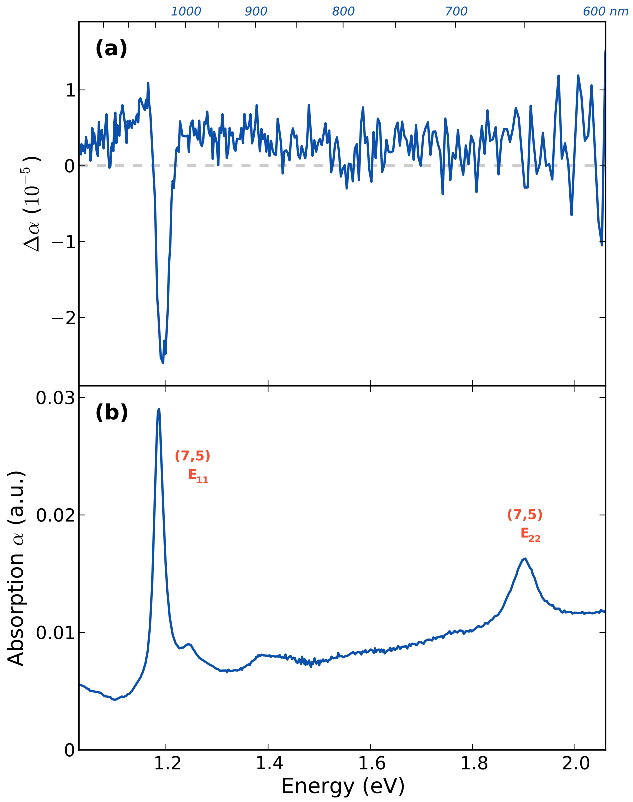

FIG. 1. (color online) Electroabsorption variation (a) and optical absorption (b) spectra of CoMoCAT/PFO extracted sample. Absorption peaks at 1.18 eV and 1.9 eV correspond respectively to E_{11} and E_{22} excitonic transitions of (7,5) SWNT. The electroabsorption spectrum was performed at a field of 12 kV/cm.

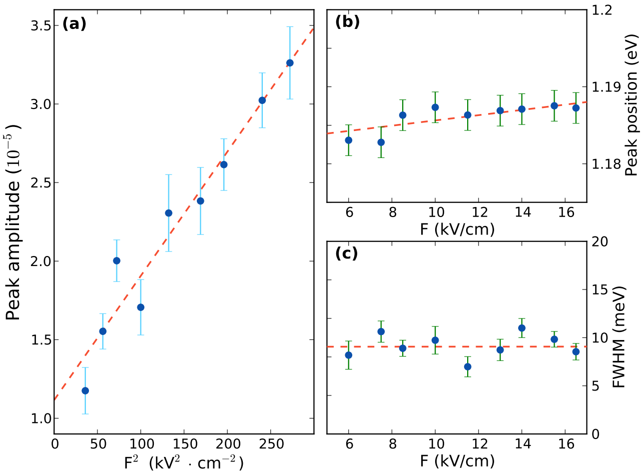

FIG. 2. (color online) Amplitude (a), position (b), and full width half maximum (FWHM) (c) as a function of the electric field applied of (7,5) SWNT electroabsorption peak in CoMoCAT/PFO extracted sample. Errors bars are the standard 2 σ deviation from the lorentzian fit, while the dashed line is the linear regression.

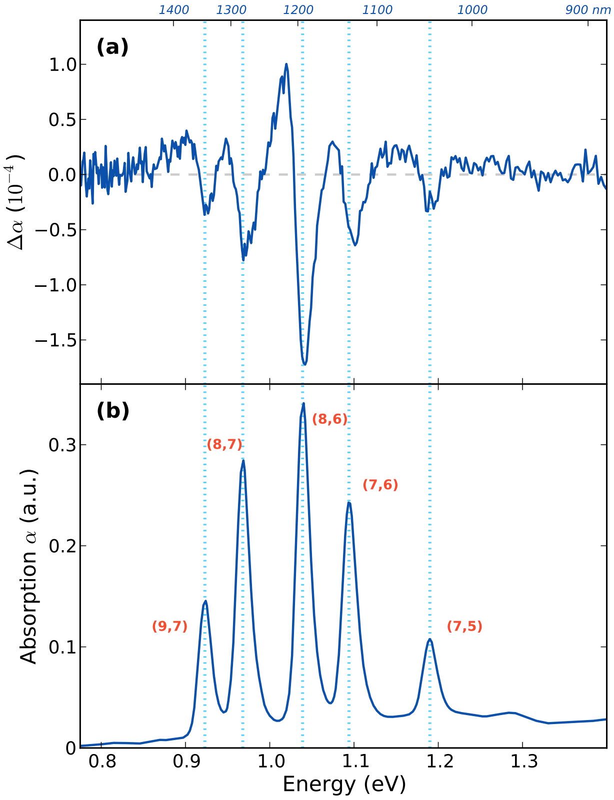

FIG. 3. (color online) Electroabsorption (a) and optical absorption (b) spectra of HiPCO/PFO extracted sample. Absorption peaks at 0.923, 0.968, 1.039, 1.094 and 1.19 eV correspond respectively to (9,7), (8,7), (8,6), (7,6) and (7,5) SWNT E_{11} excitonic transitions. The electroabsorption spectrum was performed at a field of 12 kV/cm.

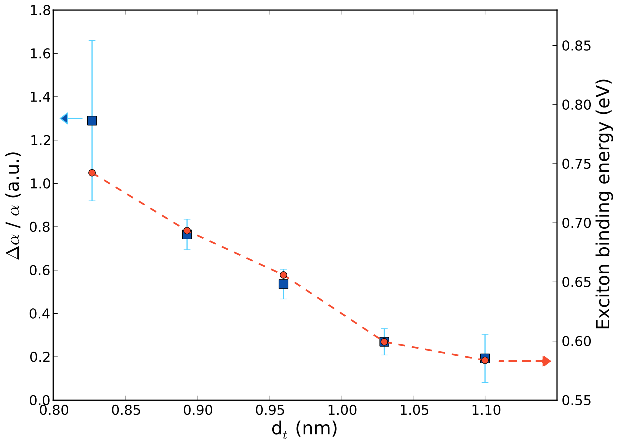

FIG. 4. (color online) Normalized electroabsorption response $\Delta\alpha/\alpha$ of HiPCO/PFO extracted nanotubes (square, left) and excitonic binding energy E_b^{11} (circle, right) as a function of the nanotube diameter d_t.